Fracture Mechanics of Concrete and Concrete Structures - High Performance, Fiber Reinforced Concrete, Special Loadings and Structural Applications- B. H. Oh, et al. (eds)

Constitutive relationships for strain-hardening cement-based composites (SHCC) subjected to tensile loading

P. Jun & V. Mechtcherine
Institute of Construction Materials, Faculty of Civil Engineering, TU Dresden, Germany

ABSTRACT: This study completes to a great extent the derivation of the constitutive relationships for Strain-Hardening Cement-based Composites (SHCC) subjected to tensile loading. These constitutive relationships are developed on the basis of a multi-scale modelling approach which considers the definitive physical phenomena observed in experimental investigations, especially in pullout tests. In previous studies by the authors, fibre pullout behaviour under monotonic as well as cyclic loading was described by a multi-linear relation. A statistical approach was used to consider the variance of the pullout response of individual fibres as observed in the experiments, where fibre embedment length and inclination served as main parameters. In this study these responses are superimposed in order to describe the stress-crack opening behaviour of each individual crack during loading, unloading, and reloading. Subsequently, characteristic stress-strain relations for SHCC under tensile loading are derived by considering an increasing number of serial cracks and the contribution of the uncracked matrix. Particular cracking behaviour is adjusted by varying the model parameters. The modelled tensile behaviour is compared with the representative results of the uniaxial tensile tests performed on the investigated SHCC and discussed.

1 INTRODUCTION

This article treats Strain-Hardening Cement-based Composites (SHCC), which display high strain capacity when subjected to tensile loading. This ductile behaviour results from progressive multiple cracking achieved by the optimised crack-bridging action of short, thin, well distributed, polymeric fibres.

The characteristic behaviour of SHCC in tension under monotonic, quasi-static loading has been studied intensively in the last few years; see Mechtcherine (2007). Mechtcherine & Jun (2007) investigated the macroscopic behaviour of SHCC under different loading regimes using deformation-controlled monotonic and cyclic tests as well as load-controlled cyclic and creep tests. Only a moderate effect of the loading regime on the tensile behaviour of SHCC was found for the set of parameters investigated.

Since the stress-strain behaviour observed at the macro-level, where the material can be assumed to be homogeneous, depends on a number of micromechanical mechanisms, a multi-scale approach is needed to develop a sound physical material model as a basis for a material law. For representative volume elements of the material, Kabele (2007) defined the stress vs. strain relationship, which considers micromechanical phenomena and further employs spatial averaging in order to link the scales of observation.

To investigate micromechanical phenomena, a series of experiments, including single-fibre tension tests, single-fibre pullout tests, and optical observations were performed by the authors; see Jun & Mechtcherine (2008). Subsequently, authors introduced the basis of a multi-scale modelling approach to derive the constitutive relations for SHCC under monotonic and cyclic tensile loading. This approach implies that the macroscopic behaviour of SHCC in the hardened state can be considered as a result of the development and joint action of multiple serial cracks, see Jun et al. (2009).

In this paper, the stress-crack opening relationship for the individual cracks is derived from the concerted action of fibres involved in crack bridging. Subsequently, the joint response of individual cracks in series and the contribution of the uncracked matrix resulting in the overall stress-strain response of SHCC exposed to tensile loading are introduced.

2 BASIS OF THE MATERIAL MODELLING

The material composition used in the related investigations by the authors was developed by Mechtcherine & Schulze (2005). The average characteristics of this material in tension were the first crack stress of 3.6MPa, tensile strength of 4.7MPa and strain capacity of 2.5%. The SHCC behaviour was investigated in displacement-controlled tests performed on

dumbbell shaped specimens with cross-section of 24mm x 40mm and the gauge length of 100mm; for further details see Mechtcherine & Jun (2007).

Jun & Mechtcherine (2008) investigated the characteristic behaviour under tension of 40μm thick and 12mm long PVA fibres used in the SHCC composition. In the same publication the results of single-fibre pullout tests are presented. The experimental program included deformation-controlled monotonic and cyclic tests. The fibres' embedded lengths varied between 1 and 6mm, with increments of 0.5mm. Typical stress-deformation response consisted of an elastic part (before full de-bonding) and a pullout part, which exhibited softening or hardening behaviour. Fibre failures could be observed in individual tests at any stage. Responses in individual tests varied significantly, even for fibres having similar embedded lengths. In order to understand this phenomenon, optical investigations using Environmental Scanning Electron Microscope (ESEM) were performed, see Jun & Mechtcherine (2008), Jun et al. (2009). The tests performed under deformation-controlled cyclic loading did not exert a pronounced effect of the loading regime on pullout behaviour. Furthermore, these tests showed consistent results with respect to the shape and inclination of the unloading and reloading branches. The shapes of the cyclic loops were not influenced by the scenario of pullout failure, i.e., fibre breakage before or after hardening, fibre pullout after hardening, or in the softening regime.

Jun et al. (2009) derived the relations for the pullout response of individual PVA fibres and for their joint action in bridging a crack. Three-dimensional, random distribution of fibres in SHCC was considered; no wall effect was taken into account. Based on this assumption, the probability density functions for the distribution of the fibres' embedded lengths and inclinations were taken from Li et al. (1991). The formula from the same reference was used to estimate the number of fibres N_f involved in crack bridging. This estimation was confirmed by the authors by visual investigation of SHCC fracture surfaces.

According to Jun et al. (2009) four basic modes could be observed in the single fibre pullout tests:

- Fibre fails before debonding from the matrix is completed;
- Fibre fails after debonding and as a consequence of fibre damage caused by friction with the inhomogeneous matrix during the hardening regime;
- Fibre is pulled out after slip hardening;
- Fibre is pulled out after complete de-bonding of fibre from matrix; no slip hardening occurs.

In very rare cases the fibre failed in the softening regime after foregoing hardening. This scenario was not considered in the modelling.

The pullout responses were described by using a number of linearly interconnected, characteristic points. Figure 1 shows a schematic response for the case with a hardening stage and a subsequent complete fibre pullout without fibre failure. This is the most "complex" curve shape of the four modes possible, and it incorporates the characteristic points of other three possible failure modes as well. The case where the fibre is broken before completion of debonding is described by one line only, following the elastic behaviour of debonded fibre's free length. Fibres broken during pullout hardening or pulled out in the softening regime without undergoing hardening at all are described by two lines. A functional description of the single fibre pullout model for all defined failure modes is given in Jun et al. (2009).

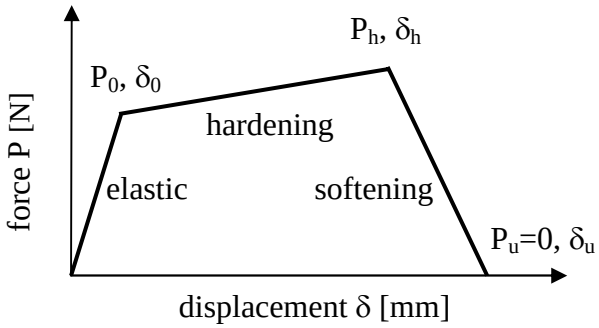

Figure 1. Schematic presentation of force-displacement curve describing fibre pullout behaviour.

Based on this description and knowing the number of bridging fibres, the pullout responses were generated within the given ranges. The number of responses generated for each specific failure scenario reflects the percentage of the corresponding responses in the experimental investigation. Fibre responses are generated only for a representative unit crack plane area of one square centimetre in order to limit the computation time. It was shown that this simplification does not influence the prediction of the material behaviour on the meso-level when larger cracked cross-sections are considered.

Because of the limitations of the pullout test setup used, the effect of fibre inclination could not be studied directly. The deviation from the vertical results in increased friction of the fibre at the edge of the cracked matrix. In order to consider the effect of fibre inclination, the approach according to Kanda & Li (1998) was adopted, see Jun et al. (2009). Further, the double-side debonding of fibre from the matrix on the both sides of the crack was considered using the approach by Wang et al. (1988).

Due to the introduction of the notion of fibre inclination and the related increase in maximum pullout force accompanied by a decrease in fibre maximum load carrying capacity, some fibres are known to change their prescribed failure mode and break before debonding and softening or hardening behaviour.

Figure 2 shows unloading-reloading loops extracted from a force-displacement diagram obtained in a cyclic fibre pullout test, see Jun et al. (2009). The figure also contains a simplified linear description of the loops.

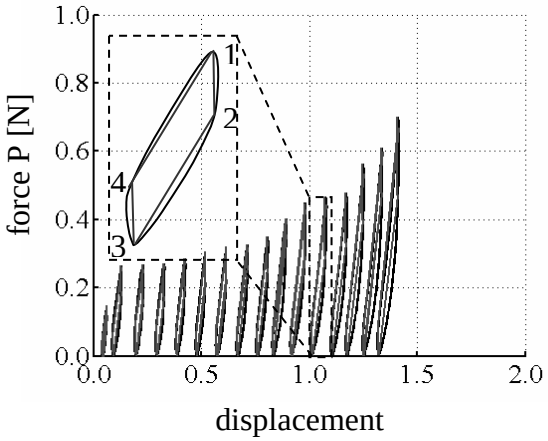

Figure 2. Unloading-reloading loops from a representative cyclic pullout test and the model description of the loops by four straight lines.

The loops were described by four points connected by straight lines. Three parameters are used to define a loop, see Jun et al. (2009). These three parameters are defined for each force level reached and approximated by linear functions by employing the method of least squares. Based on the linear dependencies observed, the shapes of the loops are defined as a function of the force reached. This procedure is further used to describe the cyclic fibre pullout behaviour.

3 DERIVATIONS OF CONSTITUTIVE RELATIONS FOR ONE CRACK

The formation and opening of merely one crack among many in SHCC is regarded as representative for the material behaviour at the meso-level. The modelling approach presented assumes that a crack is formed suddenly, through the entire cross section, and in a direction perpendicular to the loading direction. Furthermore, it is assumed that one fibre can bridge only one crack. In reality, fibres can clearly bridge more than one crack. Therefore, the newly developed crack is not necessarily bridged by fibres fully bonded in the matrix, but some of them might be debonded and being pulled out already. This phenomenon is not considered in the model.

A stress-displacement curve giving a characteristic material response at this level of observation can be derived by adding the force contributions of all fibres bridging the crack using Equation 1 and 2:

$$P(\delta)=\sum_{i=1}^{n} P_i(\delta_i) \qquad (1)$$

where P = crack bridging force, P_i = the carrying force of ith fibre as a function of dislacement δ_i, and:

$$\sigma(\delta)=\frac{P(\delta)}{A} \qquad (2)$$

where σ = tensile stress, A = the cross-section area of the tensile specimen.

Figure 3 shows a representative stress-displacement relation obtained using the procedure described above. The stress-displacement relation is within expected limits with respect to the tensile characteristics of the investigated SHCC, see Chapter 2. By varying the number of fibres involved in crack bridging action, the single-crack behaviour can be varied. However, no experimental evidence exists as yet to verify the shape of the curve directly. Therefore, at the present state of knowledge, a constitutive relationship for the entire tensile specimen has first to be derived and subsequently compared with the corresponding experimental results obtained from uniaxial tension tests on dumbbell shaped specimens in order to evaluate the accuracy of the model.

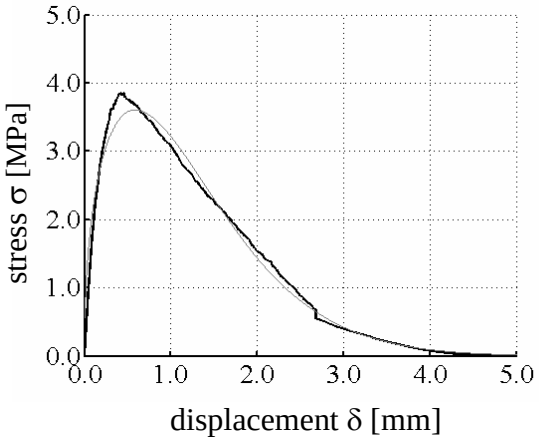

Figure 3. Modelled stress-displacement relation for one crack in SHCC (black bold line), approximation function used for modelling (grey thin line).

Figure 3 presents an approximation function for the modelled stress-displacement relation as well. Such a formula is easier to handle when the contribution of many individual cracks to the SHCC bulk behaviour is considered. The stress-deformation curve is approximated by using Equation 3:

$$\sigma(\alpha,\beta,\gamma,\delta_l)=\gamma\cdot\beta\cdot\alpha^{-\beta}\cdot(\delta_l)^{\beta-1}\cdot e^{-\left(\frac{\delta_l}{\alpha}\right)^{\beta}} \qquad (3)$$

where σ = actual tensile stress, α, β, γ = parameters, δ_l = crack opening deformation during loading (index l); the function is defined for $\delta_l > 0$.

The same approach as that used for the derivation of the stress-displacement relation for monotonic loading, i.e., adding the force contributions of a number of fibres involved in crack bridging (see above), is applied here also to determine the unloading and reloading branches during cyclic loading. Cyclic loops for individual fibres are created according to the force acting on an individual fibre at a given displacement level. The sum of all cyclic loops then creates the unloading-reloading response for one individual crack. Figure 4 shows an example of calculated unloading and reloading loops for the displacements before unloading of 0.1, 0.2, 0.3, and 0.4 mm, respectively.

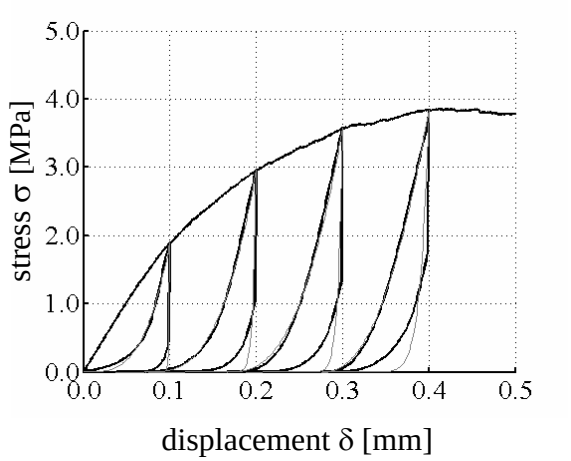

Figure 4. Modelled unloading and reloading branches of stress-displacement relation for one crack in SHCC (black bold line), approximation function used for modelling of the loops (grey thin line).

The cyclic loops derived show similar behaviour for different stress levels of the stress-displacement relation. This can be traced back to the cyclic behaviour of single fibres during the pullout test: the loops from pullout tests do not change their inclination or shape significantly with increasing displacement. The change in the inclination of loops observed on macro level (i.e. for an unnotched specimen under tensile loading), see Mechtcherine & Jun (2007), results most likely from an increasing number of cracks with increasing stress level. Equation 4 is used for the approximation of cyclic loops:

$$\sigma\left(\sigma_{\max}, \delta_{u,r}, a\right) = \sigma_{\max}\left(\delta_{u,r}\right)^{a} \tag{4}$$

where σ = actual tensile stress, σ_{max} = maximal stress before unloading, $\delta_{u,r}$= unloading (index *u*), reloading (index *r*) deformation, *a* = parameter.

4 DERIVATION OF CONSTITUTIVE RELATIONS FOR BULK MATERIAL

The overall stress-strain relationships for SHCC under tensile loading result from individual contributions of serially interconnected cracks and the contribution of the uncracked matrix. The presented model is based on an approach introduced by Kabele (2007). For modelling purposes, the behaviour of the uncracked matrix is considered to be linear-elastic, i.e. no irreversible deformations are involved. The matrix strength at the points of the prospective crack formation is randomly generated using a constant probability distribution in the value range provided by experimental results. Constitutive relations are derived under the condition of deformation control during loading, unloading and reloading.

The tensile response of SHCC can be subdivided into several stages. In the first stage, the material is loaded until the first-crack stress is reached. This stress level corresponds to the tensile strength of the weakest matrix cross-section. Since the behaviour of the uncracked matrix is considered to be linear-elastic, Equation 5 is valid also for loading, unloading and reloading of the matrix:

$$\varepsilon_{l,u,r}\left(\sigma\right) = \frac{\sigma}{E} \tag{5}$$

where $\varepsilon_{l,u,r}$ = actual strain, *l*, *u*, *r* are indices for loading, unloading and reloading stage, σ = actual tensile stress, *E* = modulus of elasticity.

With the opening of the first crack, the fibres crossing the crack are activated; from this point they transmit the tensile stresses into the cracked cross-section. The crack opens to some extent. Taking into consideration the condition of deformation control, the deformation just before and just after crack opening has to be the same. Therefore, the actual deformation of the specimen is equal to the sum of the unloading deformation of the matrix and the opening of the newly formed crack. Thus, this crack opening is determined by the unloading of the matrix, cf. Equation 5, and by the stress-deformation curve for the crack Equation 3. As a result of the steadily increasing deformation (deformation control), the overall tensile stress in SHCC drops with the opening of the first crack. The drop can be determined by solving the system of Equation 6:

$$\begin{aligned} &-\sigma_{1,d}\left(\varepsilon_{u}\right) + \sigma_{1,d}\left(\delta_{1,l}\right) = 0 \\ &-\varepsilon_{u} l_0 - \delta_{1,l} + \varepsilon_1 l_0 = 0 \end{aligned} \tag{6}$$

where $\sigma_{1,d}$ = stress after first drop, ε_u = unloading deformation of the matrix, $\delta_{1,l}$ = opening of the first crack, l_0 = gauge length of the specimen, ε_1 = actual deformation after the formation of the first crack.

Equation 5 and 3, the description of matrix unloading and the particular crack opening behaviour are established in Equation 6 and solved using the Newton-Raphson method.

As soon as the sudden stress drop is complete and the stress begins to rise again, the matrix deformation gradually increases also. Simultaneously, the newly developed crack continues opening and contributes herewith to the overall deformation. Since the carrying capacity of the fibres bridging the crack is higher than the tensile strength of the matrix in the second weakest cross-section, the scenario carries on until this strength is reached. The corresponding increase in strain can be described by Equation 7:

$$\varepsilon(\sigma) = \frac{\sigma}{E} + \frac{\delta_{1,l}(\sigma)}{l_0} \tag{7}$$

where ε = actual strain, σ = actual tensile stress, E = modulus of elasticity, $\delta_{1,l}$ = opening of 1st crack as a function of stress, l_0 = gauge length of the specimen.

When the matrix strength in the second weakest cross-section is reached, a new, second crack appears. Similarly to the situation after the formation of the first crack, the stress drops due to the new crack's opening. This drop in stress is determined as described above, with the difference that Equation 6 must be extended in order to take into account the partial closing of the first crack. In general, the ith drop associated with formation of ith crack is determined by the unloading deformation of the matrix and (i-1) cracks and by opening of the ith crack. This results in an increasing number of members of the second equation given in Equation 6, but in an increasing number of equations as well. For each additional crack opened one equation is added to the system in order to describe its unloading when the next crack is opened, (i-1) equations are added in total. The description for ith stress drop is given by Equation 8:

$$\begin{aligned} &-\sigma_{i,d}(\varepsilon_u) + \sigma_{i,d}(\delta_{i,l}) = 0 \\ &-\varepsilon_u l_0 - \delta_{i,l} + \varepsilon_i l_0 - \sum_{1}^{i-1} \delta_{i,u} = 0 \\ &-\sigma_{i,d}(\varepsilon_u) + \sigma_{i,d}(\delta_{i,u}) = 0 \end{aligned} \tag{8}$$

where $\sigma_{i,d}$ = stress after ith drop, ε_u = unloading deformation of the matrix, $\delta_{i,l}$ = opening of ith crack, l_0 = gauge length of the specimen, ε_i = actual deformation after ith crack, $\delta_{i,u}$ = partial closing of ith crack.

After each stress drop, matrix deformation starts to increase again, and simultaneously the newly developed crack is being opened. In addition, all already existing cracks reopen according to Equation 4. This scenario continues until the previous maximum stress (equal to the matrix strength at the location of the last crack) is reached. From this point, all developed cracks are being opened according to Equation 3. The overall strain can therefore be described by Equation 9 and 10:

$$\varepsilon(\sigma) = \frac{\sigma}{E} + \sum_{1_i}^{i-1} \frac{\delta_{i,r}(\sigma)}{l_0} + \frac{\delta_{i,l}(\sigma)}{l_0} \tag{9}$$

$$\varepsilon(\sigma) = \frac{\sigma}{E} + \sum_{1}^{} \frac{\delta_{i,l}(\sigma)}{l_0} \tag{10}$$

where ε = actual strain, σ = actual tensile stress, E = modulus of elasticity, $\delta_{i,r}$ = reopening of ith crack, $\delta_{i,l}$ = opening of ith crack, l_0 = gauge length of the specimen.

The formation of new cracks carries on until the strength of the next weakest cross-section is higher than the carrying capacity of fibres bridging the crack with the weakest fibre reinforcement. The failure is then localised due to the exclusive opening of this particular crack, while the stress level decreases. Equation 11 describes the material behaviour after failure localisation:

$$\varepsilon(\sigma) = -\frac{\sigma}{E} - \sum_{1}^{i-1} \frac{\delta_{i,u}(\sigma)}{l_0} + \frac{\delta_{i,l}(\sigma)}{l_0} \tag{11}$$

where ε = actual strain, σ = actual tensile stress, E = modulus of elasticity, $\delta_{i,u}$ = partial closing of ith crack, l_0 = gauge length of the specimen, $\delta_{i,l}$ = opening of ith crack.

5 RESULTS OF THE MODEL AND DISCUSSION

Figure 5 shows the modelled behaviour of SHCC under tension together with the representative response obtained from the uniaxial tension tests. Since the model generates the matrix strengths and the particular shapes of stress-crack opening relations randomly and anew every time it runs, each generated overall stress-strain response is different. The model does not prescribe the number of cracks, the procedure runs automatically and the localization occurs as soon as the corresponding criterion is satisfied. This approach enables the generation of original stress-strain relations within the limits chosen according to the experimental findings.

As can be seen from Figure 5, the stress-strain relation provided by the model conforms quite well to a representative curve obtained experimentally. With an appropriate choice of parameters, the first-crack stress and the tensile strength of the composite are in good agreement with the experimental results. However, in order to achieve correspondence of both experimental and modelled tensile strength values, the assumed behaviour of individual cracks related to the amount of bridging fibres was modified. The number of fibres acting in the "weakest crack" was enlarged by 10% and for the "strongest crack" (i.e., the crack with the strongest crack bridging by fibres) by 40%. However, since the material's performance

under tensile load is primarily governed by the weakest link, the cracked cross-section with the weakest crack bridging determines the failure. The cracks with higher carrying capacity influence the inclination of cracks' re-opening and opening branches after cracking and therefore the strain capacity of SHCC.

The single crack relations were generated to model the overall SHCC response within these enhanced limits. The need for enhancement can be explained, at least in part, by assuming a planar cracking surface as the basis for determining the fibres' amount. In the specimens tested, however, cracking surfaces were often found not to be planar but rather of more complex shapes. Thus, the number of fibres bridging a particular crack and their combined carrying capacity is likely to be higher in reality. Furthermore, the approximation used for the stress-crack opening relation for each individual crack weakens the modelled performance to some extent, see Figure 3.

The curve obtained from modelling reaches approximately the same strain capacity as measured in experiment but has fewer cracks than in the experiment. The typical measured density of visible cracks going through the entire cross-section was approximately one crack per centimetre in the case of small dumbbell specimens. For the gauge length used it means approximately 10 cracks per specimen. On examining the experimental curve more closely, more than 10 evident "jumps" can be noted, which indicates more pronounced multiple cracking. However, these additional "jumps" are of small magnitude so that they likely correspond to formation of very fine, hardly visible cracks or cracks which penetrate only a part of a specimen cross-section.

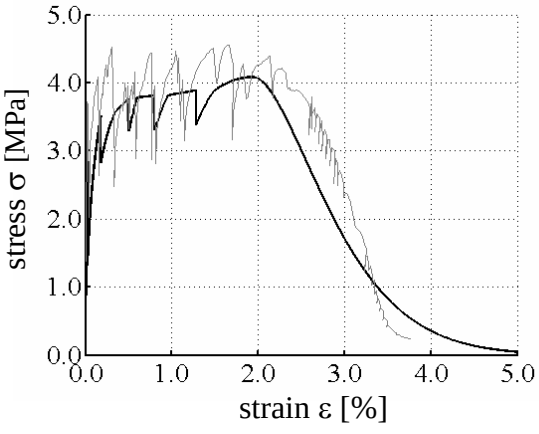

Figure 5. Modelled stress-strain relation for SHCC under monotonic tensile loading (black bold line), representative experimental result (grey thin line).

Contrarily, the modelled relation indicates formation of only 5 cracks in this particular case. Such cracking behaviour can be interpreted so if the opening of each modelled crack is accompanied by non-elastic deformations higher than those observed in the experimentation. This phenomenon again partly related to the approximation formula for stress-deformation relations used. As can be seen in Figure 3, the approximation curve exhibits a less inclined (gentler) shape around the point of maximal stress. The peak also corresponds to a higher deformation level in comparison to the originally modelled crack opening relation. The ongoing parametrical study will provide evidence if these aspects are really decisive with regard to the quality of the description of SHCC behaviour.

6 SUMMARY

The paper describes the development of constitutive relations for SHCC under tensile loading. The constitutive relationships derived consider the definitive physical phenomena investigated at different levels of observation. The results of single-fibre pullout tests are used as the basis for modelling of the material behaviour on the micro-level. Superimposing the pullout responses of all fibres involved in the crack bridging action results in a modelled stress-crack opening curve for each individual crack, including unloading and reloading behaviour. The stress-strain tensile relations for bulk SHCC are based on the joint action of the uncracked matrix and gradually developing system of cracks in serial interconnection.

The constitutive relations developed describe qualitatively and, in part, quantitatively the actual behaviour of SHCC under monotonic tensile loading. The quantitative description is to be improved further by performing a parametrical study and adjusting the model. Furthermore, the model will be extended to describe SHCC behaviour under cyclic loading.

ACKNOWLEDGEMENTS

The authors would like to thank Professor Petr Kabele (CTU Prague) for his support concerning the analytical description of the multiple cracking process in SHCC. Furthermore, thanks are extended to Mr. Jan Sykora (CTU Prague) for his help in programming the constitutive relations.

REFFERENCES

Jun, P. & Mechtcherine, V., 2008. Deformation behaviour of cracked Strain-Hardening Cement-based Composites (SHCC) under sustained and repeated tensile loading. *In: Tanabe, T. et al., Proceedings of 8th Int. Conference on Creep, Shrinkage and durability of Concrete Structure, CONCREEP 8*, Ise-Shima, Japan, Taylor & Francis Group, London, S. p. 487-493.

Jun, P., Mechtcherine. V. & Kabele. P., 2009. Derivation of a multi-scale model for Strain-Hardening Cement-based Composites (SHCC) under monotonic and cyclic tensile loading. *In: Proceedings of Int. Conference on Advanced Concrete Materials, ACM 2009*, Stellenbosch, South Africa, accepted for publication.

Kabele, P., 2007. Multiscale framework for modeling of fracture in high performance fiber reinforced cementitious composites. *Eng. Fracture Mech.*, Vol. 74, p. 194-209.

Kanda, T. & Li, V.C., 1998. Interface Property and Apparent Strength of High-Strength Hydrophilic Fiber in Cement Matrix. *J. of Materials in Civil Eng.*, Vol. 10, No. 1, p. 5-13.

Li, V.C., Wang, Y. & Backers, S., 1991. A micromechanical model of tension-softening and bridging toughening of short random fiber reinforced brittle matrix composites. *J. Mech. Phys. Solids*, Vol. 39, No. 5, p. 607-625.

Mechtcherine, V., 2007. Testing Behaviour of Strain Hardening Cement-based Composites in Tension – Summary of recent research. *RILEM-Symposium on High-Performance Fibre Reinforced Cementitious Composites HPFRCC5*, H.-W. Reinhardt and A. Naaman, RILEM PRO 53, p. 13-22.

Mechtcherine, V. & Jun, P., 2007. Stress-strain behaviour of strain-hardening cement-based composites (SHCC) under repeated tensile loading. *In: Carpinteri, A. et al. (Hrgb.), Fracture Mech. of Concrete Structures*, London: Taylor & Francis, p. 1441-1448.

Mechtcherine, V. & Schulze, J., 2005. Ultra-ductile concrete – Material design concept and testing. *Ultra-ductile concrete with short fibres – Development, Testing, Applications*, V. Mechtcherine (ed.), ibidem-Verlag, Stuttgart: p. 11-36.

Wang, Y., Li, V.C. & Backers, S., 1988. Modeling of fiber pullout from a cement matrix. *Int. J. of Cement Composites and Lightweight Concrete*, Vol. 10, No. 3, p. 143-149.